

## Article

# Removal of Heavy Metals from Contaminated Aquatic Streams Using a Resin Supported Green nZVI

Christiana Mystrioti \* and Nymphodora Papassiopi

School of Mining and Metallurgical Engineering, National Technical University of Athens, 15773 Athens, Greece; papassiop@metal.ntua.gr

\* Correspondence: chmistrioti@metal.ntua.gr; Tel.: +30-21-07724054

**Abstract:** This study addresses the escalating demand for clean water resources driven by population growth and water quality deterioration. The research focuses on evaluating the efficacy of a nanocomposite material, incorporating zero valent iron nanoparticles into a chelating cation exchange resin matrix, for selectively removing heavy metals from polluted aquatic environments. The selected resin, featuring iminodiacetic acid functional groups, demonstrates notable selectivity for heavy metal cations over alkali earth metals. Column experiments were conducted to assess the nanocomposite's performance, utilizing a feed solution spiked with heavy metals at concentrations ten times higher than Greek legislation limits for wastewater effluent recycling. The nanocomposite exhibited significant effectiveness for Cu, Cr(VI), and Pb, consistently maintaining Cu levels below detection limits and demonstrating limited breakthrough of Cr(VI) and Pb depending on experimental conditions. However, the removal efficiency was lower for Ni and insufficient for Cd, Zn, and As in this complex multicomponent solution. This research contributes valuable insights into the potential application of the developed nanocomposite for targeted removal of specific heavy metals in contaminated water sources, providing a foundation for further exploration and application in water remediation technologies.

**Keywords:** supported green nano zero valent iron (nZVI); nZVI; chelating resin; column tests; Cr(VI) and heavy metals removal; water remediation; mixed contamination



**Citation:** Mystrioti, C.; Papassiopi, N. Removal of Heavy Metals from Contaminated Aquatic Streams Using a Resin Supported Green nZVI. *Sustainability* **2024**, *16*, 1938. <https://doi.org/10.3390/su16051938>

Academic Editors: Yuanan Hu and Guannan Liu

Received: 16 November 2023

Revised: 5 February 2024

Accepted: 22 February 2024

Published: 27 February 2024



**Copyright:** © 2024 by the authors. Licensee MDPI, Basel, Switzerland. This article is an open access article distributed under the terms and conditions of the Creative Commons Attribution (CC BY) license (<https://creativecommons.org/licenses/by/4.0/>).

## 1. Introduction

The decrease and the deterioration of water resources is a significant global issue that poses a serious threat to human health and to the environment. The available deposits are dwindling while worldwide needs for drinking and clean water are expanding [1]. Sustainable treatment and reuse of wastewater effluents should be applied to meet water supply needs. Treated waters could become resources for domestic, agricultural and industrial applications.

Residual concentrations of heavy metals, such as Cr(VI), As, Ni, Pb, Cu, Cd and Zn, may exist in the effluents of industrial and urban wastewater treatment plants and if, released in the environment, may represent a real threat to human health and the ecosystem [2]. Waters polluted with various heavy metals and metalloids, with variable speciation and differing chemical properties, require combined treatment technologies to meet the stringent environmental standards and regulations. The main challenge to wastewater treatment is the development of an effective and efficient remediation treatment material that can simultaneously remove the mixed stream of multiple metals and metalloids.

Elemental iron at nanoscale proved to be an efficient medium for the treatment of contaminated waters due to its versatile properties, which combine adsorption, chemical reduction, or even Fenton type oxidation processes, and can be cleverly adapted to the specific characteristics of the target pollutants [3,4]. In particular, green nano zerovalent iron (nZVI) suspension has been thoroughly investigated for the treatment of chromates by

conducting batch, column and pilot tests [5–7]. Many studies have also demonstrated the effectiveness of this material for the removal of a wide variety of contaminants, such as heavy metals, dyes, pharmaceuticals, etc., obtaining promising results [8–10].

However, some concerns have arisen about the fate and potential ecotoxicity of iron nanoparticles in case of accidental release in aquifers. Another aspect limiting the applicability of nZVI is the difficulty of effectively separating the nanoparticles from the aqueous phase at the end of clean-up treatment [9–12]. One way to address this technological problem is to fix nanoparticles in porous materials and to use these as a permeable wall underground, if the contaminated medium is groundwater, or as a filter in above ground installations. In the last five years, our team has investigated the performance of green nano zerovalent iron (nZVI) supported on a porous matrix, such as a cationic resin, for the treatment of contaminated waters, and this iron nanocomposite, denoted as R-nZVI, has emerged as a promising alternative. This approach not only addresses the drawbacks of using pure nZVI suspension but also offers several advantages, such as high efficiency, easy application and environmentally friendly characteristics. Resin supported nanoiron (R-nZVI) is a nanocomposite material with high potential for the remediation of contaminated waters. The resin can remove cationic metal contaminants via cation exchange or chelation mechanisms, while nZVI (nano zero valent iron) is also able to remove anionic contaminants, such as Cr(VI) via reduction to Cr(III), or As(V) via adsorption on the oxidized outer shell of nZVI [13,14].

In this study, a chelating resin with iminodiacetic acid groups (Amberlite IRC748) has been evaluated as host matrix for the synthesis of R-nZVI. The performance of the nanocomposite has been evaluated for the remediation of metal contaminated waters by conducting column tests. The background solution consisted of tap water artificially contaminated with Cr(VI), As, Cu, Cd, Ni, Pb and Zn, which were examined as typical metal contaminants.

## 2. Materials and Methods

### 2.1. Synthesis of R-nZVI

The synthesis of R-nZVI nanocomposite was carried out using the resin Amberlite IRC748 (Sigma-Aldrich, Wuxi, China) as a host matrix. Amberlite IRC748 is an iminodiacetic acid chelating cation exchange resin with high selectivity for heavy metal cations over alkali metal ions found in various processes and waste streams. This selectivity is due to the iminodiacetic acid (IDA) functional groups, chemically bound to a macroreticular resin matrix (Figure 1). This type of resin was selected to obtain the selective removal of undesirable trace elements from aquatic streams, where Ca and Mg cations are often present at much higher concentration levels. The resin as received was in sodium form and is represented as  $RNa_2$  in the text.

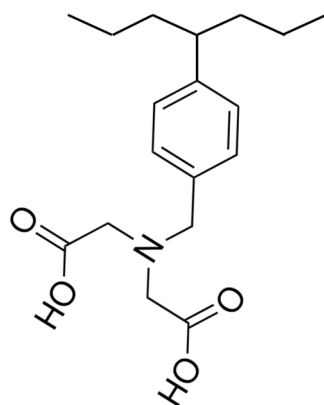


**Figure 1.** Structure of IDA functional groups in Amberlite IRC748.

Ferrous sulfate heptahydrate ( $\text{FeSO}_4 \cdot 7\text{H}_2\text{O}$ ) was used as a source of iron and dry green tea leaves (Twinings of London) as a source of polyphenols for the reduction of Fe(II) to the elemental state.

The synthesis procedure was carried out in three steps, as schematically presented in Figure 2. The first step involved mixing the resin beads ( $\text{RNa}_2$ ) with a solution containing 0.02 M Fe(II) at a  $w/v$  ratio equal to 5:100 g/mL and agitation at 100 rpm for 4 h. In the second step, the Fe(II) loaded resin (R-Fe) was treated with Green Tea (GT) extract to obtain the reduction of divalent iron to the elemental state. During this treatment, the R-Fe resin was mixed by batches of 20 g with 50 mL of GT extract and 100 mL of deionized water and agitated for 20 h. In the third step, the resin beads loaded with nZVI (R-nZVI), were mixed with 0.01 M NaCl solution ( $S/L = 1/20$  g/L) and agitated for 24 h, in order to remove the excess GT components from the internal porosity of the resin.

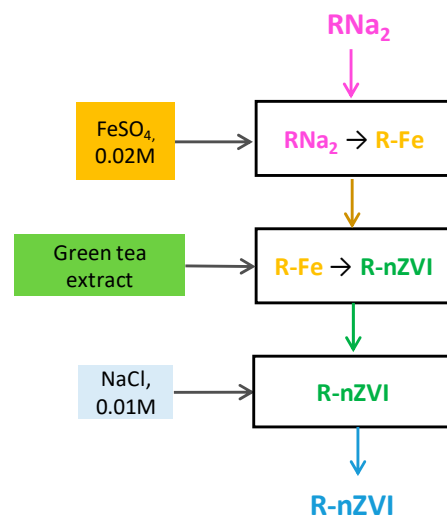


**Figure 2.** The main steps in the R-nZVI synthesis procedure.

The amount of nZVI in the resin was evaluated indirectly by mixing R-nZVI with a Cr(VI) solution in a molar ratio of approximately 1:1 and measuring the remaining Cr(VI) concentration after 4 h. The stoichiometry of reaction (1) indicates that 1 mole of Fe(0) can effectively reduce 1 mole of Cr(VI). More detailed methodology can be found in the article by Toli et al. (2016) [15]. The nZVI in the resin was found to be equal to 0.35 mmol per gram of wet resin (wR).



## 2.2. Column Tests

Column experiments were carried out using polyethylene columns, with 2.63 cm internal diameter and ~10 cm length. Column I(C) was filled with simple resin beads, which did not contain nanoiron and served as control, and the three columns, I, II and III were filled with the nanocomposite material R-nZVI. The resin beads were placed manually and gently vibrated at several stages to ensure uniform packing. In Columns I(C) and I, the resin beads occupied a height of 3 cm, and the bed volume (BV) was equal to 16.3 mL. In Columns II and III, the height of packed material was equal to 6 and 8 cm, and the bed volume was 32.6 and 43.5 mL, respectively. The detailed properties of the columns are given in Table 1.

**Table 1.** Properties of columns.

Properties Type of Resin	Columns			
	I(C) RNa <sub>2</sub>	I R-nZVI	II R-nZVI	III R-nZVI
Column diameter, d (cm)	2.63	2.63	2.63	2.63
Column height, L (cm)	3	3	6	8.0
Bed Volume, BV (cm <sup>3</sup> )	16.3	16.3	32.6	43.5
Particle density, $\rho_p$ (g/cm <sup>3</sup> )	1.10	1.15	1.15	1.15
Resin Mass, M (g)	10.2	11.2	21.8	31.8
Bulk density, $\rho_b$ <sup>(a)</sup> (g/cm <sup>3</sup> )	0.62	0.69	0.67	0.73
Porosity, $\theta$ <sup>(b)</sup>	0.43	0.40	0.42	0.36
Pore volume, $V_{PV}$ (cm <sup>3</sup> )	7.5	6.5	13.7	15.8
Flow rate, Q (mL/min)	2.5	2.5	2.5	2.5
Pore Volume Contact Time, $\tau$ <sup>(c)</sup> (min)	2.8	2.6	5.5	6.3
Empty Bed Contact Time, EBCT <sup>(d)</sup> (min)	6.5	6.5	13	17.3

<sup>(a)</sup> Dry bulk density calculated based on this equation  $\rho_b = M/BV$ , <sup>(b)</sup> Porosity calculated based on this equation  $\theta = 1 - \rho_b/\rho_p$ , <sup>(c)</sup>  $\tau = Q/V_{PV}$ , <sup>(d)</sup> EBCT =  $Q/BV$ .

The packed columns were connected to a pump and to a reservoir which contained the solutions.

The feed solution consisted of tap water, which was spiked with a concentrated solution of a mixture of heavy metals (5 mL/L) to obtain the predetermined level of metal contaminants, i.e., 500  $\mu\text{g L}^{-1}$  Cr(VI), 2  $\text{mg L}^{-1}$  Ni, 1  $\text{mg L}^{-1}$  Pb, 2  $\text{mg L}^{-1}$  Cu, 100  $\mu\text{g L}^{-1}$  Cd, 20  $\text{mg L}^{-1}$  Zn and 2  $\text{mg L}^{-1}$  As (Table 2). The concentrated solution, a mixture of heavy metals, was prepared by adding spike concentrated solutions of each contaminant. The concentrated solutions were made by dissolving solid chemical reagents in deionized water. The chemical reagents used for the preparation of concentrated solution were:  $\text{CuSO}_4 \cdot 5\text{H}_2\text{O}$  (>98%, Sigma Aldrich, Overijse, Belgium),  $\text{ZnSO}_4 \cdot 7\text{H}_2\text{O}$  (>99%, Sigma Aldrich, Overijse, Belgium),  $\text{NiSO}_4(\text{H}_2\text{O})_6$  (>98% by Merck, Darmstadt, Germany),  $\text{K}_2\text{Cr}_2\text{O}_7$  (>98% by Merck, Darmstadt, Germany),  $\text{PbSO}_4$  (>98% by Merck, Darmstadt, Belgium) and  $\text{CdSO}_4 \cdot \text{H}_2\text{O}$  (>99% by Merck, Darmstadt, Germany). As was added using an Arsenic Standard for AAS (1 g/L As in nitric acid) supplied by Sigma Aldrich, Taufkirchen, Germany.

The metal concentrations in the feed solution were selected to be approximately between five and ten times higher than the limits established by Greek legislation for recycling the effluents of municipal wastewater treatment plants in other uses [16]. Previous studies using a similar nanocomposite material have indicated that Cr(VI) removal is much more efficient at slightly acidic pHs [5]. For this reason, the pH of feed solution was adjusted to 3.5 using concentrated HCl. The composition of feed solution is shown in Table 2.

**Table 2.** Composition of feed solution.

Parameters	Feed Solution *		Upper Permitted Levels for the Reuse of Treated Waste Waters [17])
pH	3.5		
	mg/L	mmol/L	mg/L
Ca	106	2.65	
Mg	34	1.40	
Na	42	1.83	
Ni	2	0.03	0.2
Cu	2	0.03	0.2
Cd	0.1	0.0009	0.01
Zn	20	0.31	2
Pb	1	0.0048	0.1
Cr(VI)	0.5	0.0096	0.1 (total Cr)
As(V)	1.0	0.013	0.1 (total As)

\* The feed solution was analysed.

The solution was supplied from the bottom of the columns with a constant flow rate equal to 2.5 mL/min, and the same for the four columns. Taking into consideration the bed volume and the porosity of the packed beds, the contact time of the solution with the resin beads was 2.8 min in the control column, and 2.6 min, 5.5 min, and 6.3 min in the shortest, middle and highest size R-nZVI columns, respectively. The control column was kept in operation for 3 days, while the three R-nZVI columns were fed with solution for approximately 35 days.

### 2.3. Sampling and Analyses

Column effluents were sampled and analyzed for pH, EC and concentrations of hexavalent chromium, Cu, Cd, Zn, As, Ca, Mg, Ni and Pb. Cu, Ca, Mg and Zn concentrations were determined by using atomic absorption spectrometer-flame emission at Perkin Elmer PinAAcle 900T. Cd concentrations were determined by using Zeeman furnace atomic absorption spectroscopy at Perkin Elmer PinAAcle 900T (Perkin Elmer Ltd., Buckinghamshire, UK). Hexavalent chromium was analyzed by using the USEPA 7196a method, via an HACH DR-1900 spectrophotometer (HACH, Loveland, CO, USA). Arsenic concentrations were analyzed applying the ASTM D5673:2016 method at the chemical laboratory of Hellenic Survey of Geology and Mineral Exploration (H.S.G.M.E.). pH values were measured using a pH meter Metrohm 827 pH Lab. Ni and Pb were analyzed by Perkin Elmer Optima 8000 ICP-OES Inductively coupled plasma spectrometer (Perkin Elmer Ltd., Buckinghamshire, UK).

## 3. Results

### 3.1. Comparison of Nanocomposite R-nZVI with Simple $RNa_2$

#### 3.1.1. Evolution of pH

The evolution of pH in the effluents of control Column I(C) filled with simple resin beads  $RNa_2$  and column I filled with the nanocomposite R-nZVI is shown in Figure 3. The X-axis in the chart corresponds to the volume of treated solution, which is expressed as number of bed volumes ( $N_{BV}$ ) and was calculated from Equation (2):

$$N_{BV} = \frac{Q \cdot t}{V_{BV}} \quad (2)$$

where  $Q$  is the flow rate of the solution (2.5 mL/min),  $t$  is the time of operation (min) and  $V_{BV}$  is the volume occupied by the resin beads in the two columns (16.3 mL).

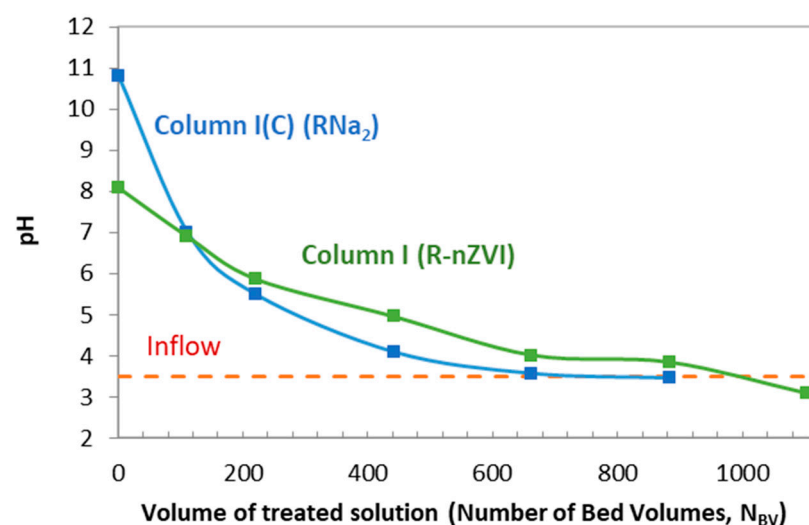


**Figure 3.** Evolution of pH in the effluents of control column I(C) filled with simple resin beads  $RNa_2$  and column I filled with the nanocomposite R-nZVI.

As seen in Figure 3, the initial pH of simple  $\text{RNA}_2$  was 10.8. and that of R-nZVI was 8.09. During the operation, the pH dropped to value 3.5 of the feed solution after the treatment with 660 BVs of solution in the control column I(C), and after 1000 BVs of solution in the R-nZVI column I.

The chelating resins with IDA functional groups have three protonated forms,  $\text{RH}_3^+$ ,  $\text{RH}_2$  and  $\text{RH}^-$ . The values of the protonation constants, as determined by Szabadka (1982), are the following:  $\log K_1 = 9.12$ ,  $\log K_2 = 3.1$ ,  $\log K_3 = 1.44$  [17]. These values were incorporated in the database of VMinteq software and were used for calculating the distribution of protonated forms as a function of pH (Figure 4).

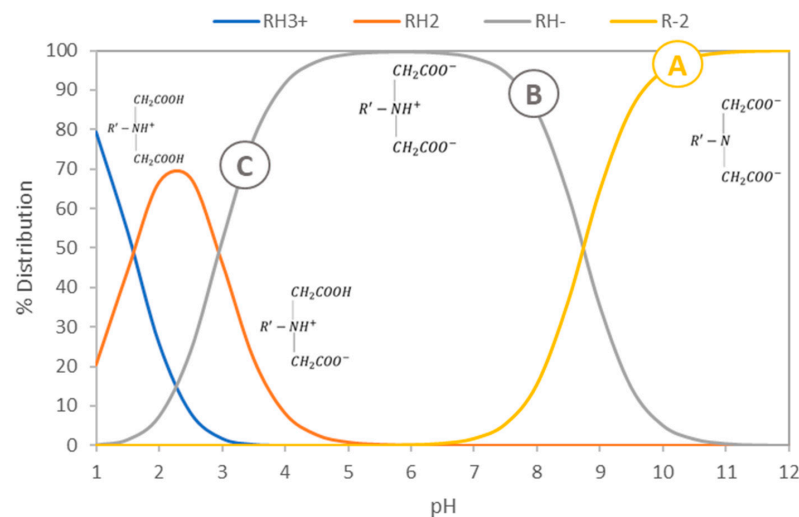


**Figure 4.** Distribution of the protonated functional groups of the iminodiacetic acid resin as a function of pH calculated using the protonation constants of Szabadka (1982) [17]. A is pH of the as received resin,  $\text{RNA}_2$ , B is pH of R-nZVI, C is pH of feed solution.

The Na form of the as received resin,  $\text{RNA}_2$ , corresponds to the fully deprotonated anion  $\text{R}^{-2}$ , which is the preponderant form of the resin above  $\text{pH} = 10$ , as seen in Figure 4. The initial  $\text{pH} = 8.1$  of the nanocomposite R-nZVI belongs to range of the monoprotonated form,  $\text{RH}^-$ , which extends between  $\text{pH} 4$  and  $8$ . At the acidic  $\text{pH} = 3.5$  of feed solution, the IDA groups of the resin are distributed between the monoprotonated and the di-protonated forms, representing 78% and 22% of total groups, respectively.

Another characteristic of the iminodiacetic functional group is that it behaves like a zwitterion, with one positive and one (or two) negative centers. The fully protonated “neutral” form,  $\text{RH}_2$ , is preponderant near  $\text{pH} 2$ . In this form, one proton of the carboxylic group is attracted by the nitrogen, creating one positive and one negative center. In the monoprotonated form  $\text{RH}^-$ , the attraction of proton by the nitrogen creates one positive center and two carboxylic anions, which are free to create chelate complexes with divalent cations.

### 3.1.2. Evolution of Cr(VI) Concentration

Amberlite IRC748 is considered a resin appropriate for the removal of cationic metal contaminants via chelation mechanisms. The main purpose of incorporating the nanoiron was to extend the applicability to other contaminants, such as the anionic species of hexavalent chromium and pentavalent arsenic.

The performances of simple resin  $\text{RNA}_2$  and nanocomposite R-nZVI for the removal of Cr(VI) are compared in Figure 5. As seen in the figure, the concentration of Cr(VI) in the effluents of the control column I(C) was similar to the concentration in the feed solution, i.e.,  $500 \mu\text{g/L}$ , during the whole operation of the column, which lasted for 5 days and corresponded to the treatment with 884 BV. This indicates that the simple resin  $\text{RNA}_2$  is not able to remove the hexavalent chromium. On the contrary, the nanocomposite material R-nZVI was very efficient in removing Cr(VI). For the same duration of treatment,

the concentration of Cr(VI) remained constantly below detection limit in the effluents of column I.

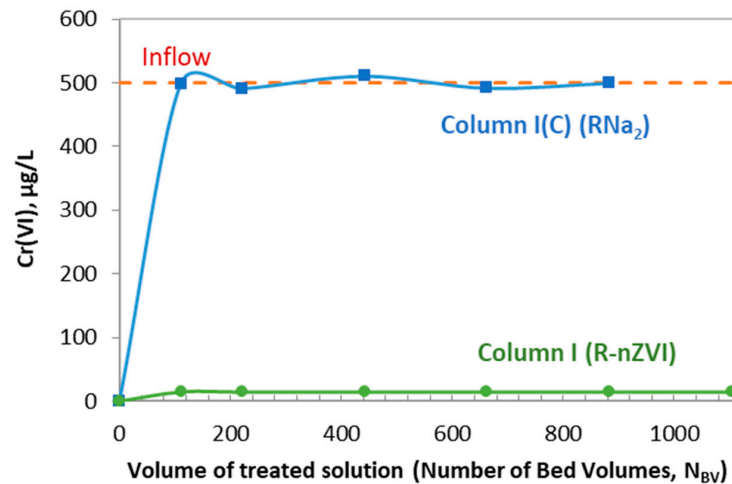
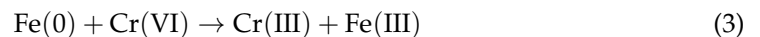


Figure 5. Evolution of Cr(VI) in the effluents of control column I(C) (RNa<sub>2</sub>) and column I (R-nZVI).

The better performance of R-nZVI for the removal of Cr(VI) can be attributed to the presence of nanoiron, which is able to reduce the Cr(VI) to the trivalent state according to the stoichiometry of reaction (3):



### 3.1.3. Evolution of As(V) Concentration

The evolution of As(V) concentration in the effluents of columns I(C) and I is shown in Figure 6. The partial retention of As(V) in the control column I(C) can be attributed to the strongly negative initial pH of the simple resin RNa<sub>2</sub>, which may have caused the precipitation of As(V) in the form of metal arsenates  $M_3(\text{AsO}_4)_2$ , where M could be the major cations  $\text{Ca}^{+2}$ ,  $\text{Mg}^{+2}$  of tap water or the spiked divalent metal cations,  $\text{Zn}^{+2}$ ,  $\text{Cd}^{+2}$ ,  $\text{Pd}^{+2}$  or  $\text{Ni}^{+2}$  [18,19]. As the water inside the column is acidified, the initially precipitated As is dissolved.

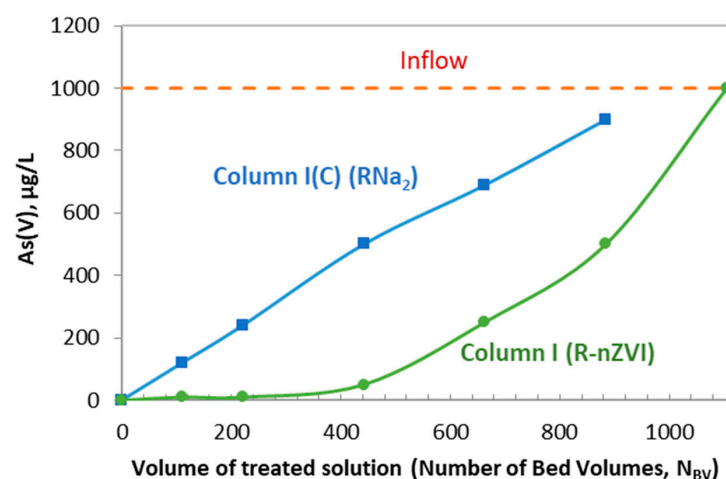
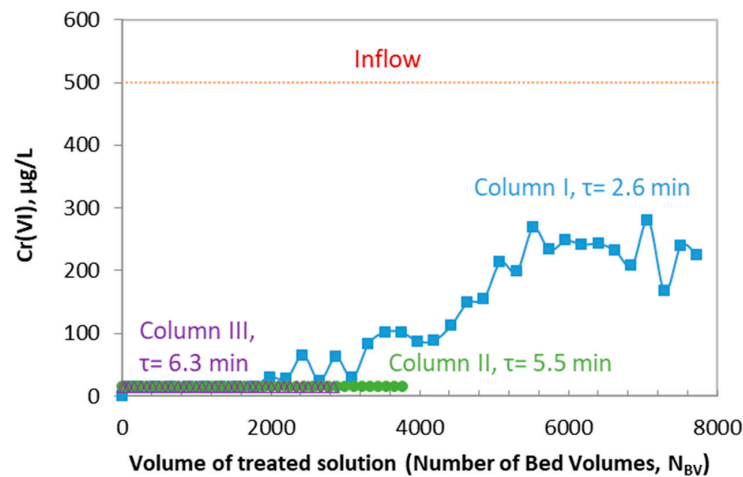


Figure 6. Evolution of As(V) in the effluents of control column I(C) (RNa<sub>2</sub>) and column I (R-nZVI).

Column I filled with the nanocomposite R-nZVI was more efficient in retaining As(V) in comparison with the control column. Arsenic was detected in the effluents after the treatment of a solution volume equivalent to 400 BVs. The amount of As retained by the nanocomposite material was equal to 0.6 mg/g.

### 3.2. Effect of Contact Time on the Removal of Cr(VI)

The effect of contact time on the concentration of Cr(VI) in the effluents of the three columns I, II and III is shown in Figure 7. The three columns were maintained in operation for 35 days with a constant flow rate of 2.5 mL/min. Due to the different height of R-nZVI in the columns, the final volume of treated solution corresponded to a different number of bed volumes for each column. Namely, the volume of treated solution was equivalent to 7730, 3780 and 2820 BVs in the short (I), middle (II) and long (III) column, respectively. On the other hand, the contact time of the solution with the nanocomposite beads was equal to 2.6, 5.5 and 6.3 min in the three columns.



**Figure 7.** Evolution of Cr(VI) concentration in the effluents of the three columns.

Chromate concentration remained below detection limit during the whole operation in the middle and long columns. It can be thus concluded that the nanocomposite material can effectively remove Cr(VI), from an initial concentration of 500 µg/L to values below 10 µg/L, for a total volume of solution equivalent to more than 3800 BVs, provided that the contact time is equal to or higher than 5.5 min (EBCT = 13 min).

In the short column (I), where the contact time was 2.6 min, the Cr(VI) was detected in the effluents after the treatment with 2000 BVs. Between 2000 and 5500 BVs, there was a gradual increase of Cr(VI) concentration. For the rest of the operation, Cr(VI) remained quasi-constant, close to 250 µg/L. This is an indication that there is a kinetic limitation to the removal of Cr(VI). Previous studies have shown that the reduction of Cr(VI) by similar nanocomposite materials follows a first order kinetics with respect to the concentration of Cr(VI) [5,20]. In this case, the inflow,  $C_{in}$ , and effluent,  $C_{ef}$ , concentrations depend on contact time, according to Equation (4):

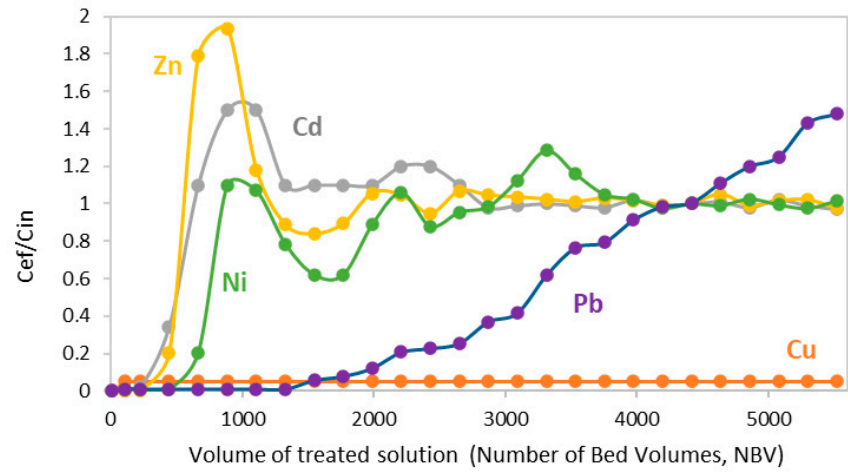
$$\ln\left(\frac{C_{ef}}{C_{in}}\right) = -k_1\tau \quad (4)$$

The value of chemical constant  $k_1$ , as calculated taking into consideration the operation data of column I between 5500 BVs and 7800 BVs, was equal to 0.267 min<sup>-1</sup>. Using this value for the chemical constant  $k_1$ , it is calculated that the minimum required contact time in order to reduce the Cr(VI) concentration from 500 µg/L to levels below the limit of 10 µg/L is equal to 14.7 min. This means that a R-nZVI column with a contact time equal to 14.7 min (EBCT = 36.6 min) would be able to operate effectively for more than 7730 BVs. The corresponding removal of Cr(VI) using this column would be more than 3790 mg Cr(VI) per L R-nZVI, or 5.6 mg per gram R-nZVI.

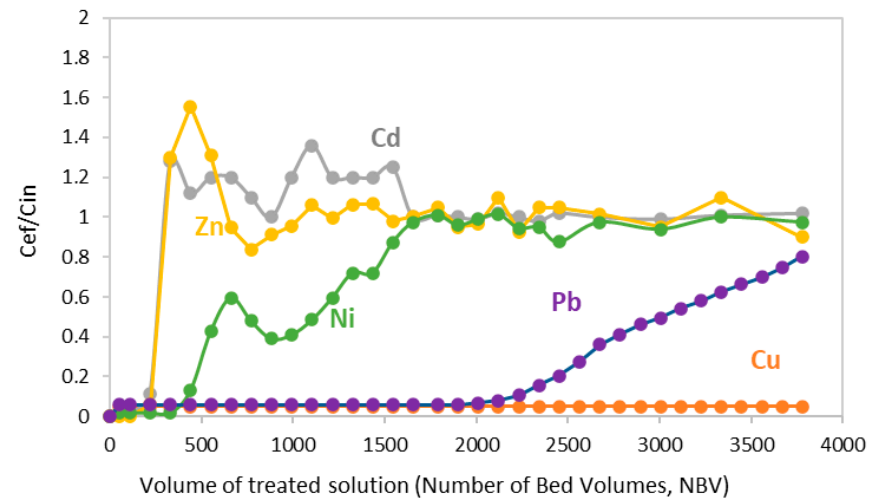
### 3.3. Removal of Cationic Contaminants

The removal of cationic contaminants in the three columns filled with R-nZVI is shown in Figure 8. The results are presented as the ratio  $C_{ef}/C_{in}$  versus the volume of

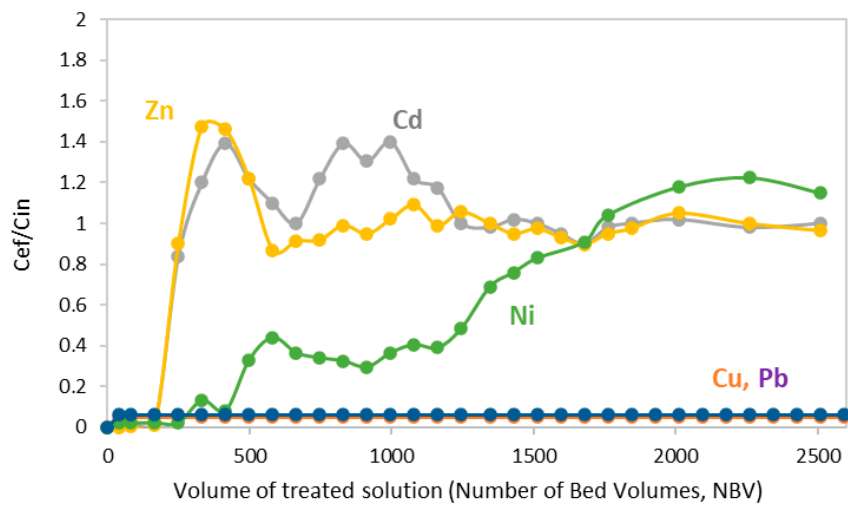
treated solution, where  $C_{ef}$  is the concentration of each element in the effluents and  $C_{in}$  the concentration in the feed solution.



(a) Column I ( $\tau = 2.6$  min)



(b) Column II ( $\tau = 5.5$  min)



(c) Column III ( $\tau = 6.3$  min)

**Figure 8.** Removal of cationic metal contaminant in the 3 columns.

As seen in Figure 8, the nanocomposite material was very efficient for the removal of Cu. The concentration of Cu in the effluents remained below detection limit during the whole operation of the three columns and in the control column. Relatively, high effectiveness was also recorded in the case of Pb. Detection of Pb in the effluents occurred after the treatment of 1550 BVs in Column I and 2120 BVs in Column II, while it was not detected during the whole operation for Column III which lasted for 2820 BVs. It is seen that the retention of Pb is improved as the contact time is increased from 2.6 min to 5.5 and 6.3 min.

Nickel appeared in the effluents after 600, 450 and 420 BVs in Columns I, II and III, respectively. Similarly, cadmium and zinc were detected after 440, 330 and 250 BVs in the three columns.

It is noted that, for a certain period of operation, the concentrations of Zn and Cd in the effluents exceeded the levels of the two elements in the feed solutions. This indicates that Zn and Cd, which were initially retained in the resin beads, were gradually expelled. Although the performance of simple resin RNa<sub>2</sub> has been specifically evaluated for the removal of cationic contaminants, its manufacturer characteristics suggest that it should be effective for the treatment of cations, with a selectivity of the following order: Na<sup>+</sup> << Ca<sup>2+</sup> < Mn<sup>2+</sup> < Fe<sup>2+</sup> < Co<sup>2+</sup> < Cd<sup>2+</sup> < Zn<sup>2+</sup> < Ni<sup>2+</sup> < Cu<sup>2+</sup> < Hg<sup>2+</sup> < Fe<sup>3+</sup>.

The evolution of pH in the effluents of the three columns is presented in Figure 9. It can be observed that the pH values of the effluents were around 3.5 after 500 BVs of treated solution.

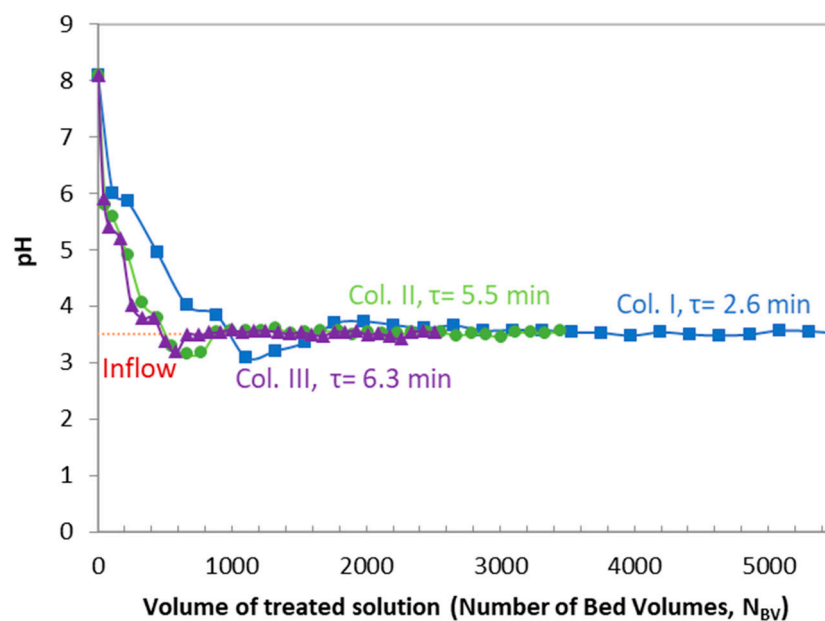


**Figure 9.** Evolution of pH in the 3 columns.

### 3.4. Fate of Major Cations, Ca<sup>2+</sup> and Mg<sup>2+</sup>

The feed solution contained Ca<sup>2+</sup> and Mg<sup>2+</sup> at higher levels in comparison with the contaminants. Namely, the concentrations of Ca and Mg were 106 and 34 mg/L, respectively, while the levels of metal contaminants ranged between 0.1 mg/L for Cd and 20 mg/L for Zn. The ratio C<sub>ef</sub>:C<sub>in</sub> for Ca and Mg in the effluents of column II is shown in Figure 10. The two elements were initially retained in the resin, but they were rapidly displaced by the protons and by the other cations exhibiting higher affinity for the iminodiacetic groups. A similar trend was observed in the other two columns.

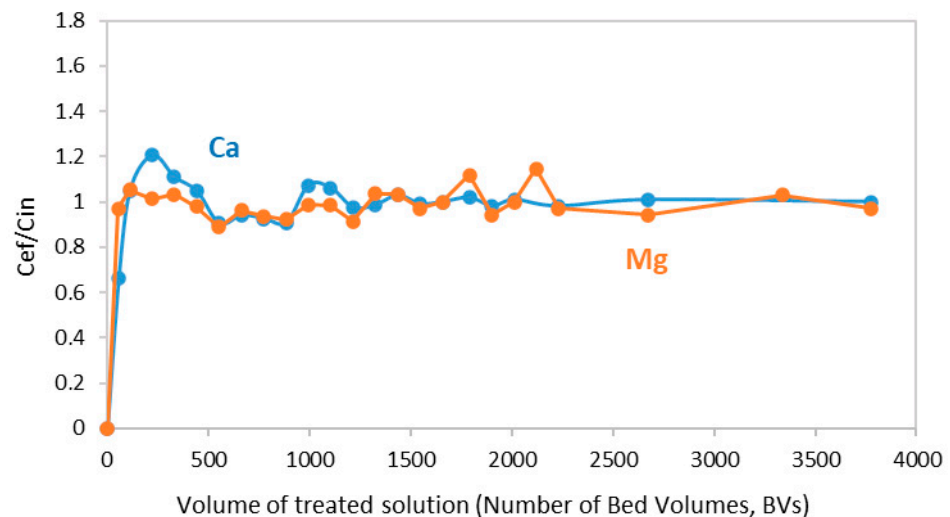


**Figure 10.** Evolution of  $C_{ef}:C_{in}$  ratio for Ca and Mg in the effluents of Column II.

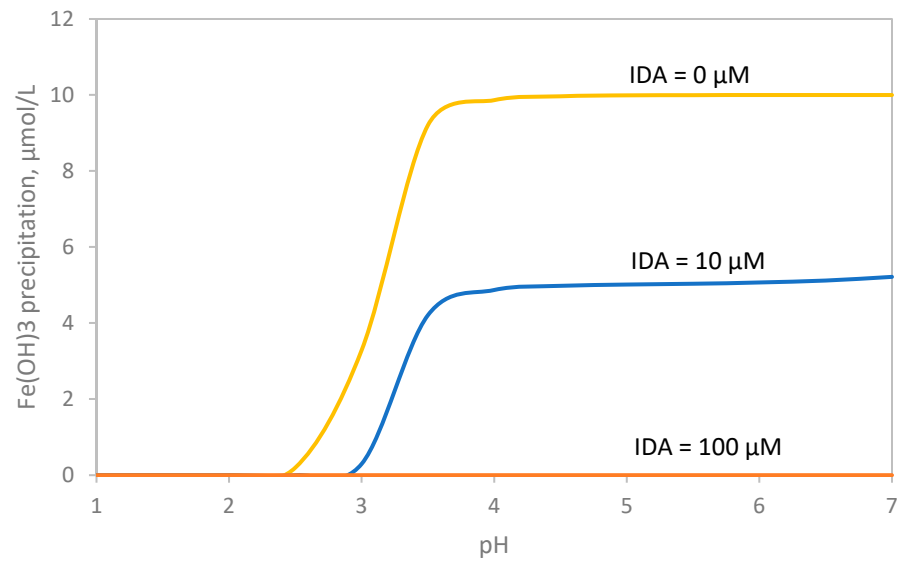
### 3.5. Effect of Iminodiacetic Acid Resin

The matrix used for the incorporation of nZVI was the chelating cation exchange resin Amberlite IRC748, where the functional groups are iminodiacetic acid. In this type of resin, the tertiary nitrogen atom is attached to the polymer chain and the two carboxyl groups are available for the formation of chelates with divalent and trivalent cations. Depending on the pH, the functional groups may have partially or fully protonated forms, as already shown in Figure 4. This resin was selected because it exhibits a strong selectivity for heavy metals with respect to alkaline earth cations.

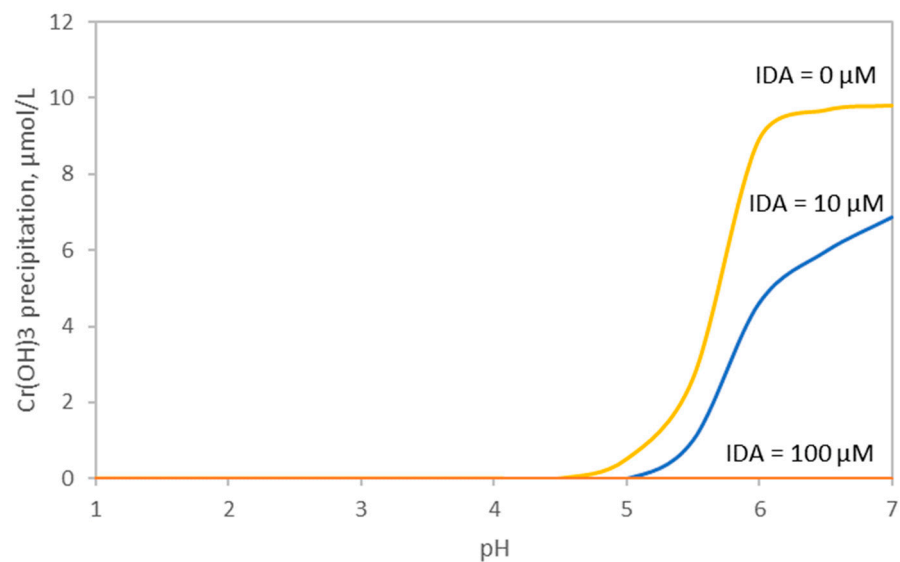
The nanocomposite was found to be very efficient for the removal of Cu and Cr(VI). The main mechanism involved in the removal of Cu was chelation by the iminodiacetic groups of the resin. For Cr(VI), the preponderant mechanism was reduction to trivalent state by the nZVI nanoparticles.

As shown in Equation (2), the reduction of Cr(VI) by the elemental iron results in the production of Cr(III) and Fe(III) cations. At  $pH > 3.5$  and in the absence of chelating ligands, Fe(III) precipitates as  $Fe(OH)_3$ . Precipitation of Cr(III) in the form of single or mixed Fe(III)-Cr(III) hydroxides, e.g.,  $(xCr(OH)_3 (1 - x) Fe(OH)_3)$ , occurs at slightly higher pH values, e.g.,  $pHs > 4.5$  [20]. In the presence of chelating ligands, such as iminodiacetic acid, the ligands form very strong chelates with Fe(III) and Cr(III) and may hinder the precipitation of the corresponding hydroxides.

The effect of iminodiacetic acid ligands on the precipitation of Fe(III) and Cr(III) hydroxides is shown in Figure 11. The diagrams present the amount of precipitated  $Fe(OH)_3$  and  $Cr(OH)_3$ , as a function of pH, from solutions containing  $10 \mu M$  Fe(III) or Cr(III) and various concentrations of iminodiacetic acid (IDA) 0, 10 and  $100 \mu M$ . Calculations were carried out using the software Visual Minteq V3.2. Formation constants for Fe(III)-IDA chelates and for Cr(III)-IDA chelates were obtained from the bibliography and are given in the Supplementary Material (Table S1) [21,22]. As seen in Figure 11a, in the absence of IDA, precipitation of  $Fe(OH)_3$  starts at pH 2.5 and is complete at  $pH > 4$ . In the presence of IDA at equimolar concentration with Fe of  $10 \mu M$ , precipitation starts at pH 3 and when the pH increases only above 50% of the Fe precipitates. When IDA is present in excess, at  $100 \mu M$ , all Fe(III) remains in solution. A similar trend is observed for  $Cr(OH)_3$  in Figure 11b. The main difference is that precipitation of the hydroxide starts close to pH 4.5 without IDA and pH 5.0 with  $10 \mu M$  IDA. Based on above calculations, it is estimated that the trivalent cations, Fe(III) and Cr(III), which were produced from the reduction of hexavalent chromium by the nanoiron, were probably retained by chelation in the iminodiacetic acid functional groups of the resin.



(a) Fe(III)



(b) Cr(III)

**Figure 11.** Precipitation of  $\text{Fe}(\text{OH})_3$  and  $\text{Cr}(\text{OH})_3$  as a function of pH from solutions containing  $10 \mu\text{M}$  Fe(III) or Cr(III) and various concentrations of iminodiacetic acid (IDA), IDA = 0, 10 and  $100 \mu\text{M}$ .

### 3.6. Comparative Presentation of the Results

The results obtained for all the examined contaminants are presented in Table 3. To evaluate the performance of treatment for each specific contaminant, the following parameters are presented in the Table: (i) the maximum volume of solution per volume of bed,  $N_{\text{BV}}$ , for which the contaminant is removed at levels below detection limit; (ii) the corresponding contact time, expressed as pore volume,  $\tau$ , and empty bed, EBCT, contact time; and (iii) the corresponding loading of R-nZVI bed,  $q_{\text{B}}$  expressed as mg of contaminant per liter of bed.

**Table 3.** R-nZVI performance for all examined contaminants.

	Cr(VI)	Cr(VI)	As(V)	Cu	Pb	Pb	Ni	Cd	Zn
Inflow concentration, $C_{in}$ (mg/L)	0.5	0.5	1	2	1	1	2	0.1	20
Outflow concentration, $C_{ef}$ (mg/L)	<0.010	<0.010	<0.010	<0.1	0.05	<0.05	<0.04	<0.001	<0.06
Volume of treated solution with successful removal, $N_{BV}$ (L/L bed) *	3800	7730	400	>7800	2120	>2820	600	440	440
Contact time, $t$ (min)	5.5	14.7	2.6	2.6	5.5	6.3	2.6	2.6	2.6
Empty bed contact time, EBCT (min)	13	37	6.5	6.5	13	17	6.5	6.5	6.5
RnZVI loading $q_B$ (mg/L) **	1900	3790	400	>15,600	2120	>2820	1200	44	8800

\* Volume of treated solution with successful removal of the specific contaminant with concentrations in the outflow below detection limit,  $N_{BV}$  (L of solution/L of bed) \*\*  $q_B = N_{BV} \cdot C_{in}$ .

The effectiveness of R-nZVI for the removal of contaminants from this aquatic stream with mixed contamination followed the order:

$$Cu > Cr(VI) > Pb > Ni > Cd \sim Zn > As(V)$$

The removal of copper was very effective. With the lowest tested contact time of  $\tau = 2.6$  min (EBCT 6.5 min), it was possible to remove Cu from an amount of solution exceeding 7800 L per liter of RnZVI bed. The corresponding loading was more than 15,600 mg Cu per liter of bed.

The removal of Cr(VI) was found to depend on contact time. With  $\tau = 5.5$  min (EBCT = 13 min), it was possible to effectively treat 3800 L per liter of bed. It was estimated that, if the contact time was increased to 14.7 min (EBCT = 37 min), the effective treatment could be extended to 7700 L per liter of bed and the removal of Cr(VI) from 1900 to 3790 mg per bed liter.

A kinetic limitation was also observed regarding Pb removal. When the contact time was 5.5 min, the effective treatment of solution lasted for 2120 bed volumes. When the contact volume increased to 6.3 min, there was an extension to more than 2820 bed volumes.

For Ni, the effective treatment lasted for 600 L per liter of bed, with RnZVI loading equal to 1200 mg/L. For Cd and Zn, the corresponding performance was 440 L per bed liter and the loading of bed was equal to 44 mg Cd and 8800 mg Zn per bed liter.

The removal of As(V) was limited to the initial 400 L per liter of bed and the RnZVI loading was equal to 400 mg per liter of bed.

#### 4. Discussion

The nanocomposite material Rn-nZVI synthesized in the framework of this study consisted of elemental iron nanoparticles (nZVI) incorporated in a chelating cation exchange resin. The performance of this nanocomposite was evaluated for the remediation of an aquatic solution contaminated with a mixture of contaminants, i.e., Cr(VI), Ni, Pb, Cu, Cd, Zn and As. To have an estimation for potential competition of coexisting major elements, like Ca and Mg, the background solution consisted of tap water. Both the resin host matrix and nZVI particles contributed to the removal of metals.

The reactivity of nZVI is primarily related to the strong reducing capacity of elemental iron. Metallic iron can theoretically reduce to the elemental state and immobilize all the metal cations with a higher standard reduction potential (see Table 4). It can also reduce many oxyanions, like  $CrO_4^{-2}$ , which are soluble in their oxidized and insoluble in their reduced form. A second important mechanism of nZVI reactivity is due to its core-shell structure of nZVI. When the metallic iron nanoparticles come in contact with the aquatic environment, their surface is oxidized and a layer of iron oxides is rapidly formed around the metallic core. The iron oxides shell provides a very efficient substrate for the adsorption of contaminants. As shown in Table 3 the maximum estimated amount of reduced Cr(VI) in the R-nZVI bed, when the contact time is close to 15 min, is equal to 3790 mg/L, or 5.6 mg per gram nZVI.

**Table 4.** Selectivity factors of Amberlite IRC748 for metal cations at pH = 4, as provided by the manufacturer.

	Cu <sup>+2</sup>	Pb <sup>+2</sup>	Ni <sup>+2</sup>	Zn <sup>+2</sup>	Cd <sup>+2</sup>	Fe <sup>+2</sup>	Ca <sup>+2</sup>
K = M/Ca	2300	1200	57	17	15	4.0	1.0

In previous studies, which were carried out with a similar nanocomposite product, it was found that the removed Cr(VI) was almost equimolar with the iron incorporated in the resin beads. This performance was obtained from batch experiments and using solutions containing only Cr(VI) in deionized water [23]. In the present study, the synthesized R-nZVI contained 0.35 mmol nZVI per gram of resin. Therefore, the theoretical maximum removal of Cr(VI) could be as high as 18 g/(g R-nZVI). However, the possible practical loading of this resin is not expected to be as high, due to the mixed contamination and the complex matrix of treated solution.

In other publications where elemental nanoiron was incorporated in granular polymeric matrices, the maximum removal of Cr(VI) was reported to range between 1 and 4 mg/g [24–26]. Higher Cr(VI) removal rates, in the range 40–60 mg/g, have been determined in some recent studies, where nZVI was supported on matrices with fine particle size distribution, such as the mineral schwertmannite [27] or finely ground activated biochar [28]. However, these types of material are not appropriate for use in filter installations, due to their fine particle size.

Based on the findings of many published studies, arsenic was also expected to be removed from the aqueous solution due to the presence of nZVI [29–34]. In these studies, nZVI was supported on several matrices, such as activated carbon, montmorillonite, graphite oxide, fuller's earth etc., and the total removal capacity was reported to range between 10 and 100 mg of As per gram of composite material. The proposed mechanisms of As removal were (i) adsorption on the layer of iron oxides and hydroxides formed around the metallic core of ZVI, and (ii) precipitation of ferric and ferrous arsenate phases, like scorodite, FeAsO<sub>4</sub>·2H<sub>2</sub>O, and symplectite, Fe<sub>3</sub>(AsO<sub>4</sub>)<sub>2</sub>·8H<sub>2</sub>O.

The nanocomposite material tested in our study presented a much lower performance for the removal of As, compared to the previously reported studies. Namely, the maximum amount of As(V) retained by the R-nZVI during the operation of the columns was close to 0.6 mg/g. This is probably related to the specific properties of the resin, used as supporting matrix for the ZVI nanoparticles. As already discussed, the iminodiacetic functional groups of the resin can form very strong complexes with Fe(III) cations and may have hindered the formation of the iron hydroxide shell around the metallic core of the nanoparticles. As a consequence, the appropriate substrate for the adsorption of As oxyanions is missing. On the other hand, precipitation of ferric and ferrous arsenates is not expected to contribute to the removal of As, due to the acidic pH of the inflow solution and the competitive action of iminodiacetic groups.

The observed selectivity of R-nZVI for the examined metal cations, i.e., Cu<sup>+2</sup>, Pb<sup>+2</sup>, Ni<sup>+2</sup>, Zn<sup>+2</sup>, Cd<sup>+2</sup>, is in accordance with the selectivity of Amberlite IRC748, as reported by the manufacturer (Table 5). In the technical data sheet, it is also reported that the affinity for H<sup>+</sup> at pH 4 is situated between Cu<sup>+2</sup> and Pb<sup>+2</sup> [35]. This can explain the ejection of Zn and Cd from the resin when the pH dropped below 4.

**Table 5.** Standard reduction potential of metal cations to the respective elemental state.

	Cu <sup>+2</sup> /Cu <sup>0</sup>	Pb <sup>+2</sup> /Pb <sup>0</sup>	Ni <sup>+2</sup> /Ni <sup>0</sup>	Cd <sup>+2</sup> /Cd <sup>0</sup>	Fe <sup>+2</sup> /Fe <sup>0</sup>	Zn <sup>+2</sup> /Zn <sup>0</sup>
E <sub>h</sub> <sup>0</sup> (V)	0.34	−0.13	−0.25	−0.40	−0.44	−0.76

In the nanocomposite material R-nZVI, the removal of metal contaminants may be also related to the presence of elemental iron. The standard reduction potentials, E<sub>h</sub><sup>0</sup>, of the elements of concern are presented in Table 5. As seen in Table 5, the values of E<sub>h</sub><sup>0</sup> for Cu<sup>+2</sup>, Pb<sup>+2</sup> and Ni<sup>+2</sup> are higher than that of Fe<sup>+2</sup>, the E<sub>h</sub><sup>0</sup> of Cd<sup>+2</sup> is close to that of Fe<sup>+2</sup>,

and the  $Eh^0$  of  $Zn^{+2}$  is more negative. Theoretically,  $Cu^{+2}$ ,  $Pb^{+2}$  and  $Ni^{+2}$  can be reduced to the elemental state by metallic Fe nanoparticles, while Cd and Zn are not expected to be affected by the presence of nZVI.

## 5. Conclusions

Summarizing the finding of this work, the synthesized nanocomposite material R-nZVI was found to be an effective medium for the simultaneous removal of Cr(VI), Cu and Pb from contaminated waters. It was also demonstrated that the major cations, Ca and Mg, though present at much higher concentrations, did not affect the removal of contaminants. The nanocomposite was less efficient in the case of Ni, Cd, Zn and As. R-nZVI versatility allows it to be incorporated into various treatment systems, including advanced oxidation processes (AOPs), electrocoagulation (EC), fixed-bed reactors, membrane filtration, landfill leachate treatment, oil–water separation, desalination, pharmaceutical wastewater treatment, municipal wastewater treatment, and industrial wastewater treatment [36]. Further research is needed to fully explore their potential in wastewater treatment applications.

**Supplementary Materials:** The following supporting information can be downloaded at: <https://www.mdpi.com/article/10.3390/su16051938/s1>, Figure S1: Precipitation of  $Fe(OH)_3$  and  $Cr(OH)_3$  as a function of pH from solutions containing 10  $\mu M$  Fe(III) or Cr(III) and various concentrations of iminodiacetic acid (IDA), IDA = 0, 10 and 100  $\mu M$ ; Table S1: IDA complexes as incorporated in VMinteq databases; Table S2: Complexes of N-Benzylamine-DA.

**Author Contributions:** Conceptualization, N.P.; methodology, N.P.; validation, C.M.; formal analysis, C.M.; investigation, C.M.; resources, C.M.; data curation, N.P.; writing—original draft preparation, C.M.; writing—review and editing, C.M.; visualization, C.M.; supervision, N.P.; project administration, C.M. All authors have read and agreed to the published version of the manuscript.

**Funding:** This research received no external funding.

**Institutional Review Board Statement:** Not applicable.

**Informed Consent Statement:** Not applicable.

**Data Availability Statement:** Data are contained within the article.

**Conflicts of Interest:** The authors declare no conflicts of interest.

## References

1. WHO; UNICEF; World Bank. *State of the World's Drinking Water: An Urgent Call to Action to Accelerate Progress on Ensuring Safe Drinking Water for All*; World Health Organization: Geneva, Switzerland, 2022.
2. Tchounwou, P.B.; Yedjou, C.G.; Patlolla, A.K.; Sutton, D.J. Heavy metal toxicity and the environment. *Exp. Suppl.* **2012**, *101*, 133–164. [PubMed]
3. Gao, Y.; Yang, X.; Lu, X.; Li, M.; Wang, L.; Wang, Y. Kinetics and Mechanisms of Cr(VI) Removal by nZVI: Influencing Parameters and Modification. *Catalysts* **2022**, *12*, 999. [CrossRef]
4. Zhu, F.; Ma, S.; Liu, T.; Deng, X. Green synthesis of nano zero-valent iron/Cu by green tea to remove hexavalent chromium from groundwater. *J. Clean. Prod.* **2018**, *174*, 184–190. [CrossRef]
5. Sathya, S.; Ragul, V.; Veeraraghavan, V.P.; Singh, L.; Ahamed, N. An in vitro study on hexavalent chromium [Cr(VI)] remediation using iron oxide nanoparticles based beads. *Environ. Nanotechnol. Monit. Manag.* **2020**, *14*, 100333. [CrossRef]
6. Zhu, F.; Liu, T.; Zhang, Z.; Liang, W. Remediation of hexavalent chromium in column by green synthesized nanoscale zero-valent iron/nickel: Factors, migration model and numerical simulation. *Ecotoxicol. Environ. Saf.* **2021**, *207*, 111572. [CrossRef]
7. Conde-Cid, M.; Paiga, P.; Moreira, M.M.; Albergaria, J.T.; Álvarez-Rodríguez, E.; Arias-Estévez, M.; Delerue-Matos, C. Sulfadiazine removal using green zero-valent iron nanoparticles: A low-cost and eco-friendly alternative technology for water remediation. *Environ. Res.* **2021**, *198*, 110451. [CrossRef] [PubMed]
8. Delnavaz, M.; Kazemimofrad, Z. Nano zerovalent iron (nZVI) adsorption performance on acidic dye 36 removal: Optimization of effective factors, isotherm and kinetic study. *Environ. Prog. Sustain. Energy* **2020**, *39*, 3349. [CrossRef]
9. Tarekegn, M.M.; Hiruy, A.M.; Dekebo, A.H. Nano zero valent iron (nZVI) particles for the removal of heavy metals ( $Cd^{2+}$ ,  $Cu^{2+}$  and  $Pb^{2+}$ ) from aqueous solutions. *RSC Adv.* **2021**, *11*, 18539–18551. [CrossRef] [PubMed]
10. Shi, Z.; Fan, D.; Johnson, R.L.; Tratnyek, P.G.; Nurmi, J.T.; Wu, Y.; Williams, K.H. Methods for characterizing the fate and effects of nano zerovalent iron during groundwater remediation. *J. Contam. Hydrol.* **2015**, *181*, 17–35. [CrossRef] [PubMed]

11. Zeng, G.; He, Y.; Wang, F.; Luo, H.; Liang, D.; Wang, J.; Huang, J.; Yu, C.; Jin, L.; Sun, D. Toxicity of Nanoscale Zero-Valent Iron to Soil Microorganisms and Related Defense Mechanisms: A Review. *Toxics* **2023**, *11*, 514. [[CrossRef](#)] [[PubMed](#)]
12. Xue, W.; Huang, D.; Zeng, G.; Wan, J.; Cheng, M.; Zhang, C.; Hu, C.; Li, L. Performance and toxicity assessment of nanoscale zero valent iron particles in the remediation of contaminated soil: A review. *Chemosphere* **2018**, *210*, 1145–1156. [[CrossRef](#)]
13. Hubicki, Z.; Kołodziejka, D. Selective Removal of Heavy Metal Ions from Waters and Waste Waters Using Ion Exchange Methods. *Ion Exch. Technol.* **2012**, *7*, 193–240. [[CrossRef](#)]
14. Aredes, S.; Klein, B.; Pawlik, M. The removal of arsenic from water using natural iron oxide minerals. *J. Clean. Prod.* **2012**, *29–30*, 208–213. [[CrossRef](#)]
15. Toli, A.; Chalastara, K.; Mystrioti, C.; Xenidis, A.; Papassiopi, N. Incorporation of zero valent iron nanoparticles in the matrix of cationic resin beads for the remediation of Cr(VI) contaminated waters. *Environ. Pollut.* **2016**, *214*, 419–429. [[CrossRef](#)] [[PubMed](#)]
16. Greek legislation: FEK 354/B/2011.
17. Szabadka, O. Studies on chelating resins -II Determination of the protonation constants of a chelating resin containing iminodiacetic acid groups. *Talanta* **1982**, *29*, 183–187. [[CrossRef](#)]
18. Bothe, J.; Brown, P. The stabilities of calcium arsenates at  $23 \pm 1$  °C. *J. Hazard. Mater.* **1999**, *B69*, 197–207. [[CrossRef](#)]
19. Lee, J.; Nriagu, J. Stability constants for metal arsenates. *Environ. Chem.* **2007**, *4*, 123–133. [[CrossRef](#)]
20. Chebeir, M.; Liu, H. Oxidation of Cr(III)-Fe(III) Mixed-Phase Hydroxides by Chlorine: Implications on the Control of Hexavalent Chromium in Drinking Water. *Environ. Sci. Technol.* **2018**, *52*, 7663–7670. [[CrossRef](#)]
21. Sanchiz, J.; Esparza, P.; Domínguez, S.; Brito, F.; Mederos, A. Solution studies of complexes of iron(III) with iminodiacetic, alkyl-substituted iminodiacetic and nitrilotriacetic acids by potentiometry and cyclic voltammetry. *Inorganica Chim. Acta* **1999**, *291*, 158–165. [[CrossRef](#)]
22. Mizuochi, H.; Shirakata, S.; Kyuno, E.; Tsuchiya, R. Chromium(III) Complexes with Iminodiacetic Acid or *l*-Aspartic Acid. *Bull. Chem. Soc. Jpn.* **1970**, *43*, 397–400. [[CrossRef](#)]
23. Poguberović, S.S.; Krčmar, D.M.; Maletić, S.P.; Kónya, Z.; Tomašević Pilipović, D.D.; Kerkez, D.V.; Rončević, S.D. Removal of As(III) and Cr(VI) from aqueous solutions using “green” zero-valent iron nanoparticles produced by oak, mulberry and cherry leaf extracts. *Ecol. Eng.* **2016**, *90*, 42–49. [[CrossRef](#)]
24. Ponder, S.M.; Darab, J.G.; Mallouk, T.E. Remediation of Cr(VI) and Pb(II) Aqueous Solutions Using Supported, Nanoscale Zero-valent Iron. *Environ. Sci. Technol.* **2000**, *34*, 2564–2569. [[CrossRef](#)]
25. Fu, F.; Ma, J.; Xie, L.; Tang, B.; Han, W.; Lin, S. Chromium removal using resin supported nanoscale zero-valent iron. *J. Environ. Manag.* **2013**, *128*, 822–827. [[CrossRef](#)] [[PubMed](#)]
26. Huang, J.F.; Li, Y.T.; Wu, J.H.; Cao, P.Y.; Liu, Y.L.; Jiang, G.B. Floatable, macroporous structured alginate sphere supporting iron nanoparticles used for emergent Cr(VI) spill treatment. *Carbohydr. Polym.* **2016**, *146*, 115–122. [[CrossRef](#)] [[PubMed](#)]
27. Xie, Y.; Lu, G.; Tao, X.; Wen, Z.; Dang, Z. A collaborative strategy for elevated reduction and immobilization of Cr(VI) using nano zero valent iron assisted by schwertmannite: Removal performance and mechanism. *J. Hazard. Mater.* **2022**, *422*, 126952. [[CrossRef](#)]
28. Zhuang, M.; Wang, H.; Qi, L.; Cui, L.; Quan, G.; Yan, J. Production of activated biochar via a self-blowing strategy-supported sulfidated nanoscale zerovalent iron with enhanced reactivity and stability for Cr(VI) reduction. *J. Clean. Prod.* **2021**, *315*, 128108. [[CrossRef](#)]
29. Baikousi, M.; Georgiou, Y.; Daikopoulos, C.; Bourlinos, A.B.; Filip, J.; Zboril, R.; Deligiannakis, Y.; Karakassides, M.A. Synthesis and characterization of robust zero valent iron/mesoporous carbon composites and their applications in arsenic removal. *Carbon* **2015**, *93*, 636–647. [[CrossRef](#)]
30. Bhowmick, S.; Chakraborty, S.; Mondal, P.; Van Renterghem, W.; Van den Berghe, S.; Roman-Ross, G.; Chatterjee, D.; Iglesias, M. Montmorillonite-supported nanoscale zero-valent iron for removal of arsenic from aqueous solution: Kinetics and mechanism. *Chem. Eng. J.* **2014**, *243*, 14–23. [[CrossRef](#)]
31. Morgada, M.E.; Levy, I.K.; Salomone, V.; Farias, S.S.; Lopez, G.; Litter, M.I. Arsenic (V) removal with nanoparticulate zerovalent iron: Effect of UV light and humic acids. *Catal. Today* **2009**, *143*, 261–268. [[CrossRef](#)]
32. Nakseedee, P.; Tanboonchuy, V.; Pimpha, N.; Khemthong, P.; Liao, C.-H.; Gridanurak, N. Arsenic removal by nanoiron coupled with gas bubbling system. *J. Taiwan Inst. Chem. Eng.* **2015**, *47*, 182–189. [[CrossRef](#)]
33. Yadav, R.; Sharma, A.K.; Babu, J.N. Sorptive removal of arsenite [As(III)] and arsenate [As(V)] by fuller’s earth immobilized nanoscale zero-valent iron nanoparticles (F-rZVI): Effect of Fe<sup>0</sup> loading on adsorption activity. *J. Environ. Chem. Eng.* **2016**, *4*, 681–694. [[CrossRef](#)]
34. Zhu, H.; Jia, Y.; Wu, X.; Wang, H. Removal of arsenic from water by supported nano zero-valent iron on activated carbon. *J. Hazard. Mater.* **2009**, *172*, 1591–1596. [[CrossRef](#)]
35. Kheskwani, U.; Ahammed, M.M. Removal of water pollutants using plant-based nanoscale zero-valent iron: A review. *Water Sci. Technol.* **2023**, *88*, 1207–1231. [[CrossRef](#)] [[PubMed](#)]
36. Marini, L.; Acconero, M. Prediction of the thermodynamic properties of metal-arsenates and metal-arsenite aqueous complexes to high temperature and pressures and some geological consequences. *Environ. Geol.* **2007**, *52*, 1343–1363. [[CrossRef](#)]

**Disclaimer/Publisher’s Note:** The statements, opinions and data contained in all publications are solely those of the individual author(s) and contributor(s) and not of MDPI and/or the editor(s). MDPI and/or the editor(s) disclaim responsibility for any injury to people or property resulting from any ideas, methods, instructions or products referred to in the content.